

Supporting Information

Biodegradable PEG-Dendritic Block Copolymers: Synthesis and Biofunctionality Assessment as Vectors of siRNA

Victoria Leiro*,†,‡, João Pedro Garcia†,‡,§, Pedro M.D. Moreno†,‡, Marcos Fernandez-Villamarin[⊥], Ricardo Riguera[⊥], Eduardo Fernandez-Megia*,[⊥]
and Ana Paula Pêgo*,†,‡,§,||

* i3S - Instituto de Investigação e Inovação em Saúde and ‡ INEB – Instituto de Engenharia Biomédica, Universidade do Porto, Rua Alfredo Allen, 208, 4200-135 Porto, Portugal; § Faculdade de Engenharia da Universidade do Porto (FEUP), and || Instituto de Ciências Biomédicas Abel Salazar (ICBAS) - Universidade do Porto, Porto, Portugal

⊥ Department of Organic Chemistry and Center for Research in Biological Chemistry and Molecular Materials (CIQUS), University of Santiago de Compostela, Jenaro de la Fuente s/n, 15782 Santiago de Compostela, Spain

Table of Contents

	Page
1) ^1H and ^{13}C NMR spectra	3
2) MALDI-TOF spectrum for PEG-b[G2]-N ₃ (G2) (9)	14
3) FTIR Transmittance spectra	15
4) Degradability studies	16
5) Stability of the dendriplexes in different media	18
6) Heparin dissociation assay	20
7) Dendriplexes degradation studies	20
8) Internalization data	21

1) ^1H and ^{13}C NMR Spectra (Solvent peaks labeled as * in spectra)

tert-butyl gallate (2)

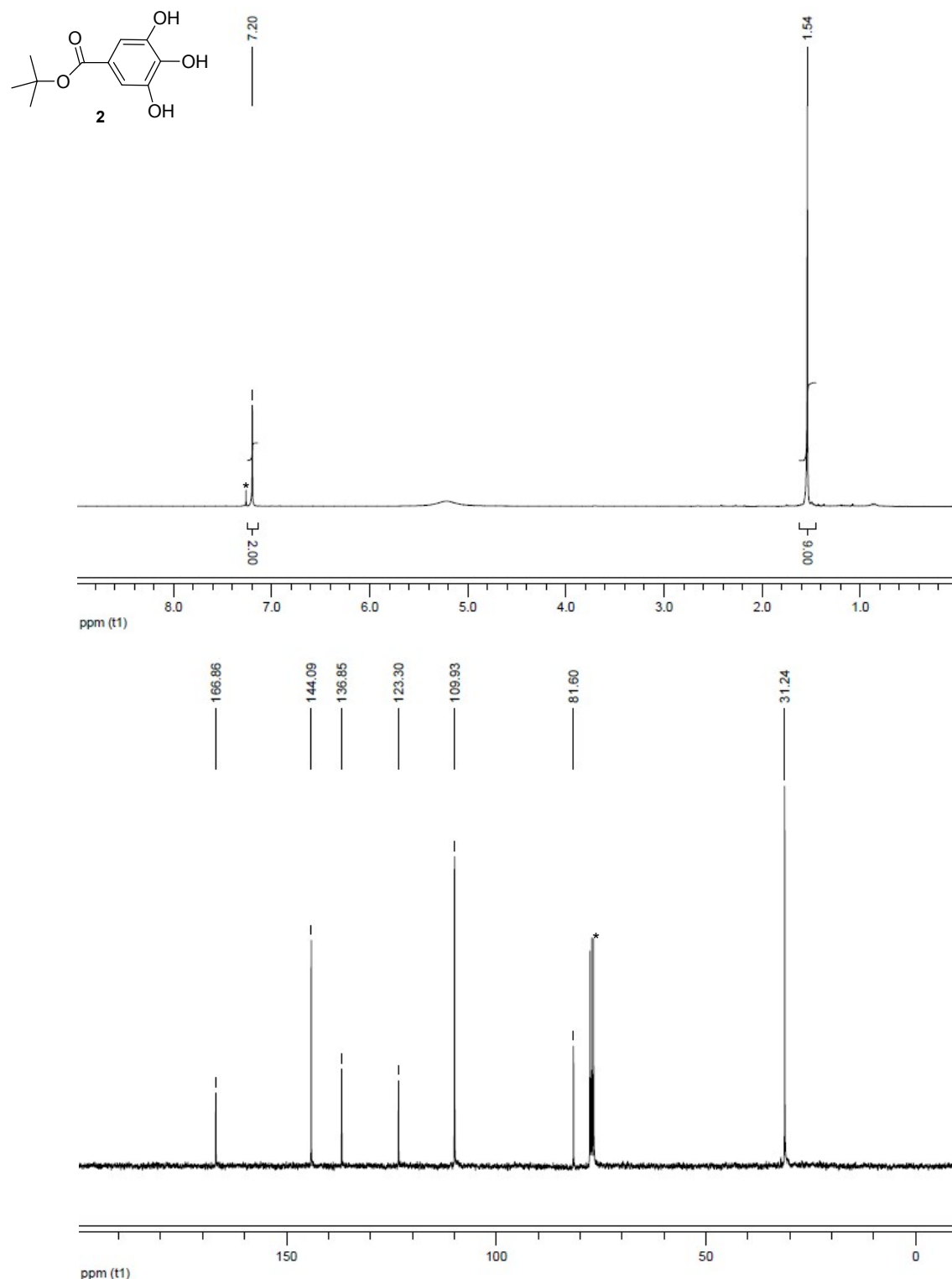


Figure S1. ^1H and ^{13}C NMR Spectra of **2**

2-[2-(2-azidoethoxy)ethoxy]ethyl 4-bromobutanoate (4)

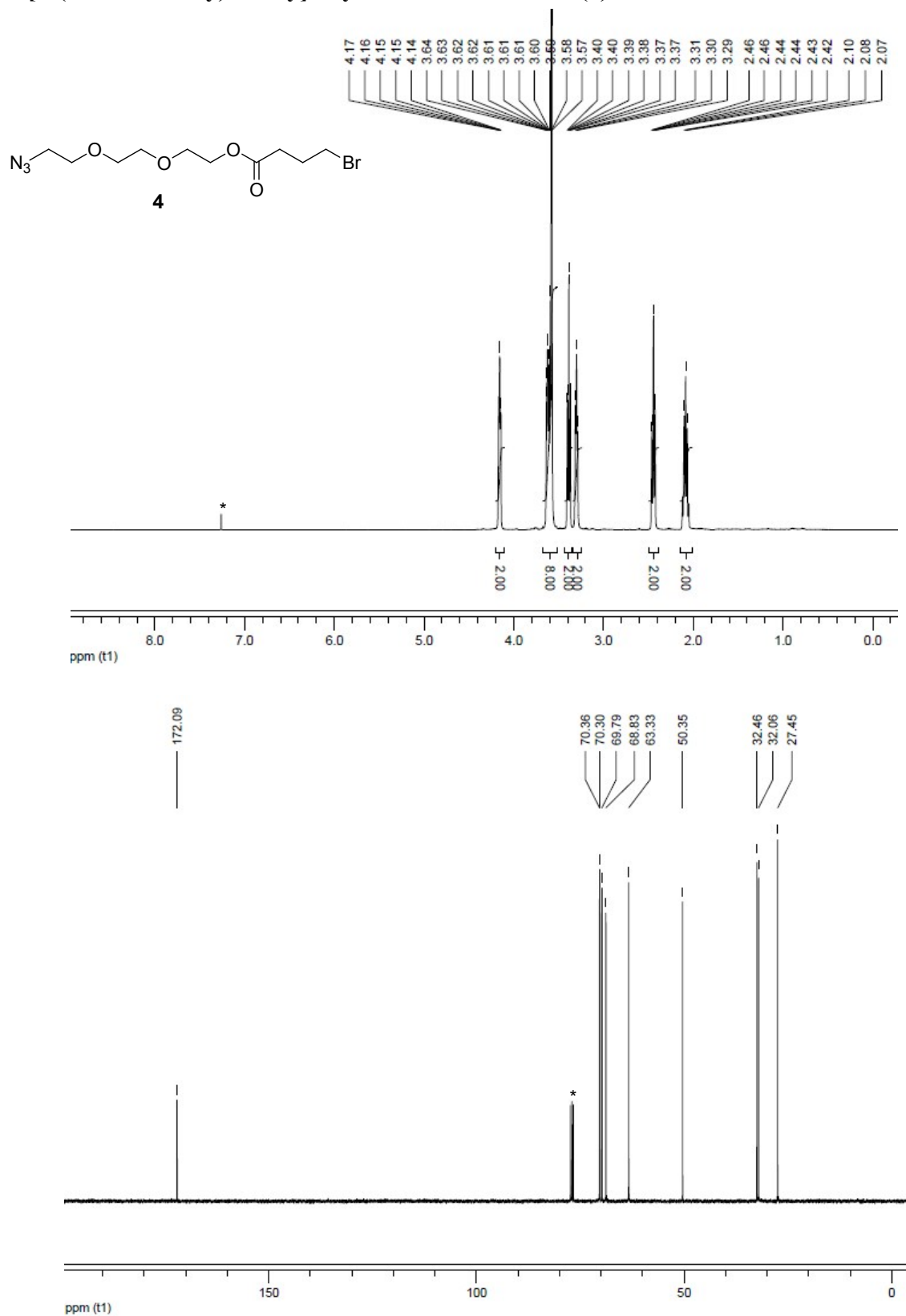


Figure S2. ^1H and ^{13}C NMR spectra of 4

Tris{2-[2-(2-azidoethoxy)ethoxy]ethyl} 4,4',4''-{[5-(tert-butoxycarbonyl)benzene-1,2,3-triyl]tris(oxy)}tributanoate

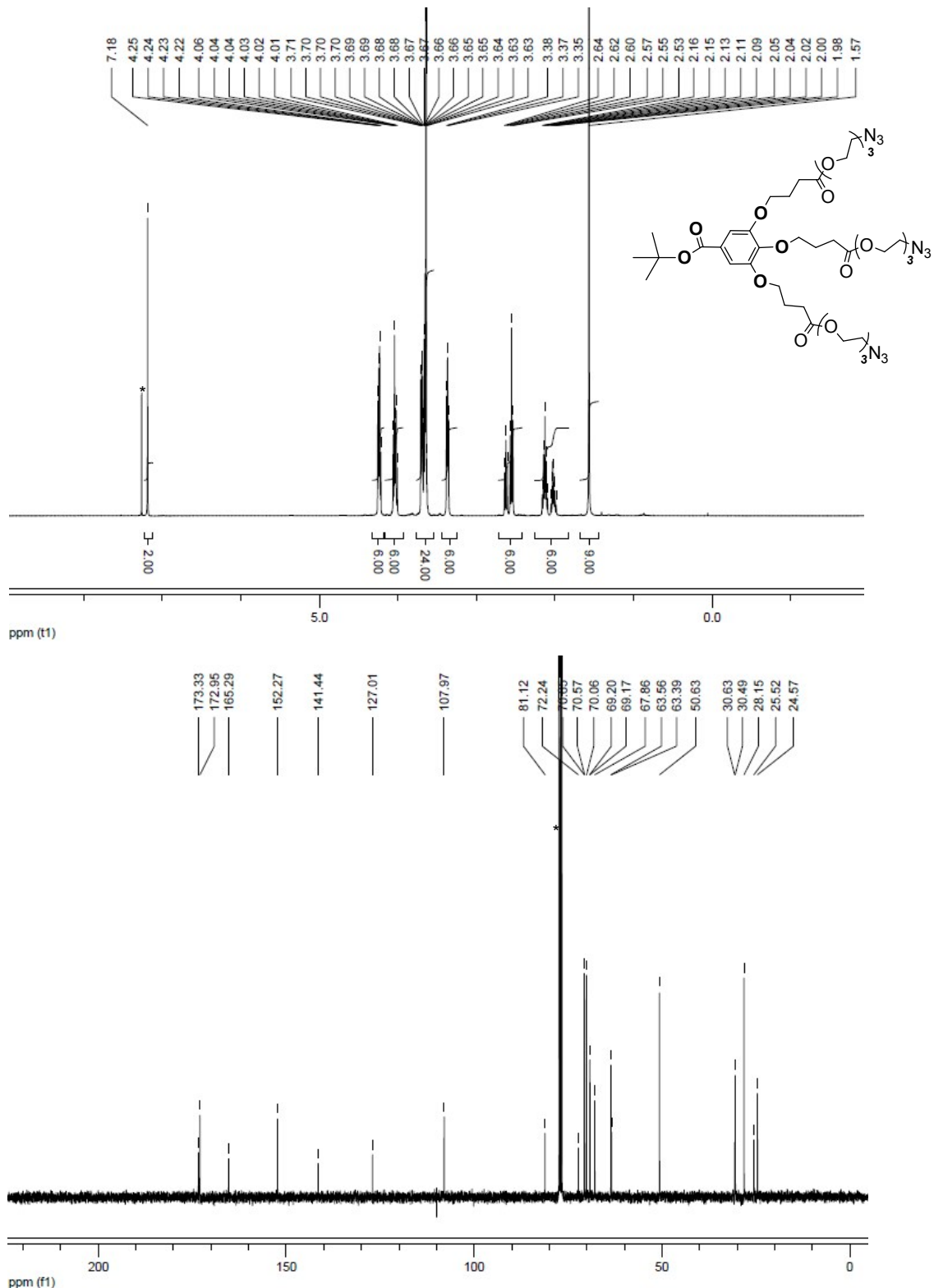


Figure S3. ^1H and ^{13}C NMR spectra of tris{2-[2-(2-azidoethoxy)ethoxy]ethyl} 4,4',4"-{[5-(tert-butoxycarbonyl)benzene-1,2,3-triyl]tris(oxy)} tributanoate

**3,4,5-tris(4-{2-[2-(2-azidoethoxy)ethoxy]ethoxy}-4-oxobutoxy)benzoic acid (5)
(GATGE buiding unit)**

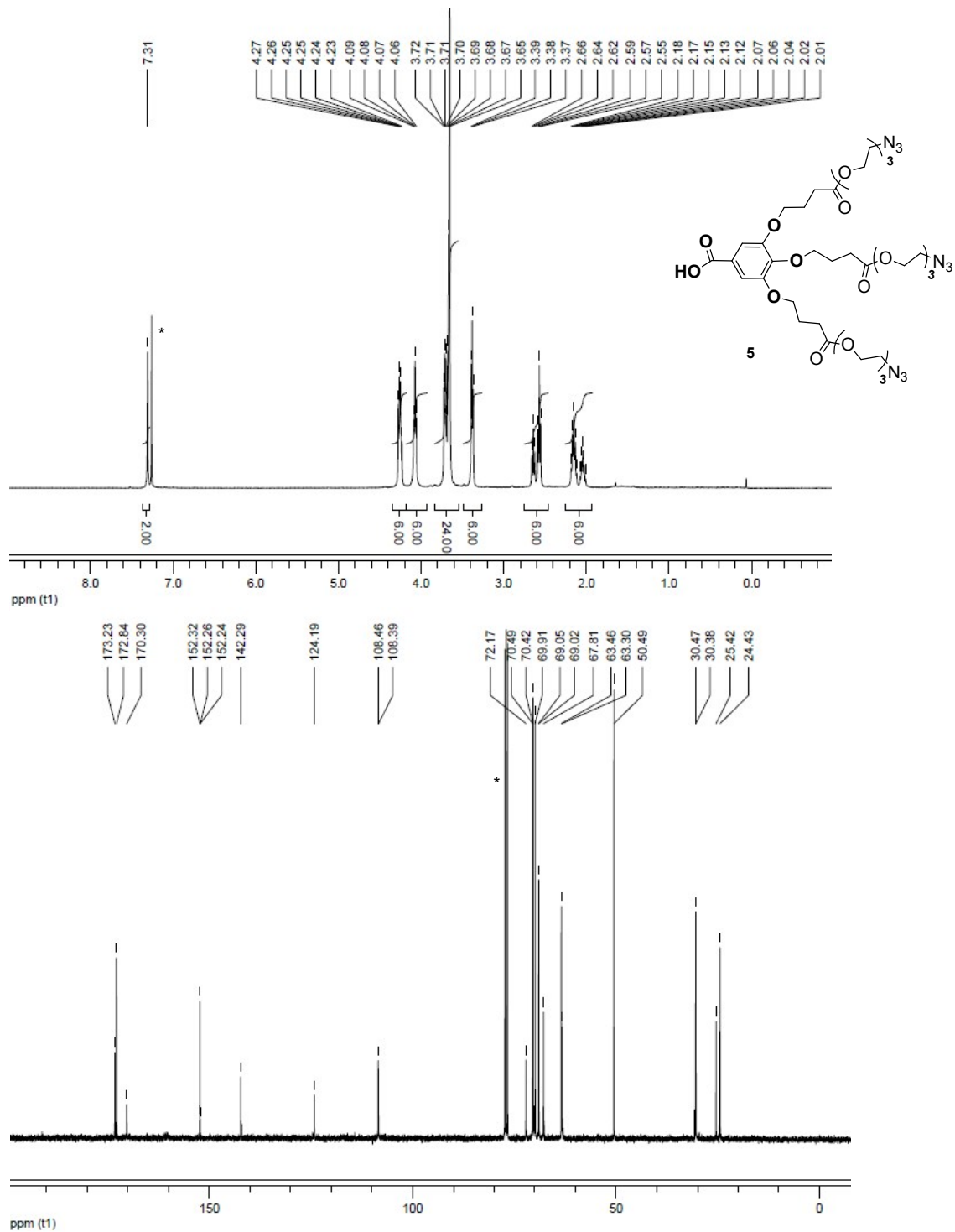


Figure S4. ^1H and ^{13}C NMR spectra of **5**

PEG-[G1]-N₃ (8)

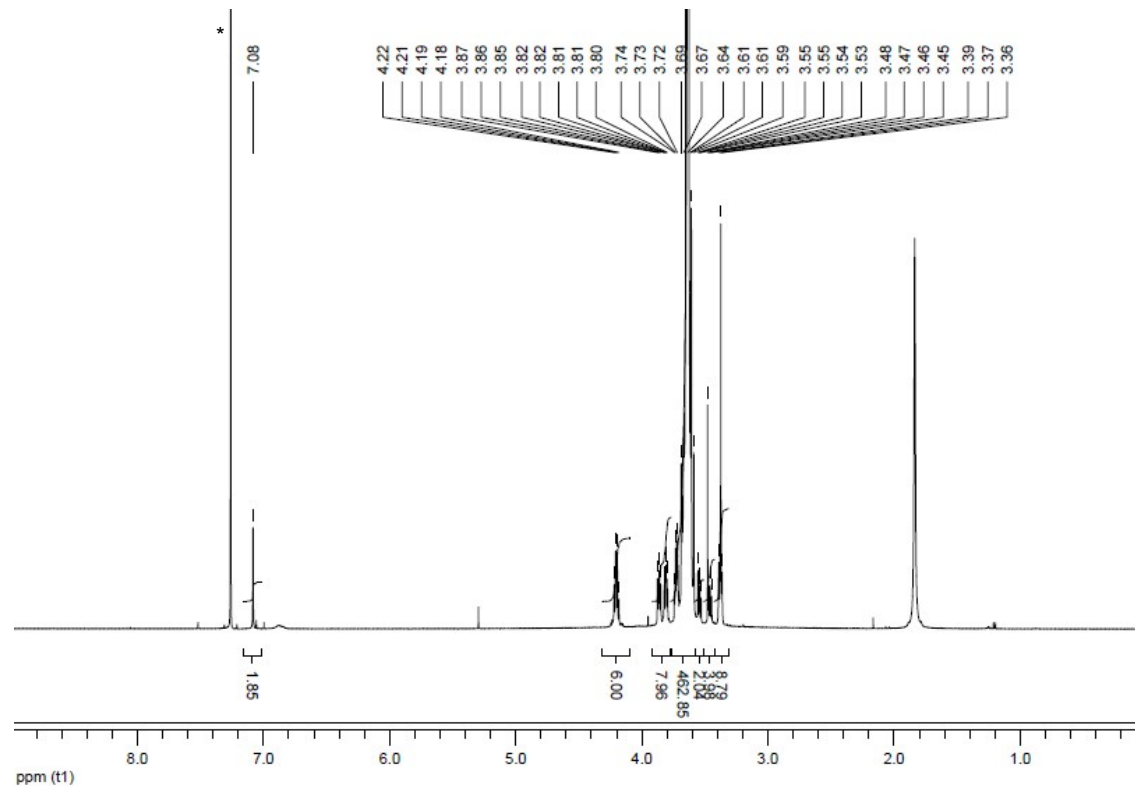


Figure S5. ¹H NMR spectrum of PEG-[G1]-N₃ (8)

PEG-[G1]-NH₂

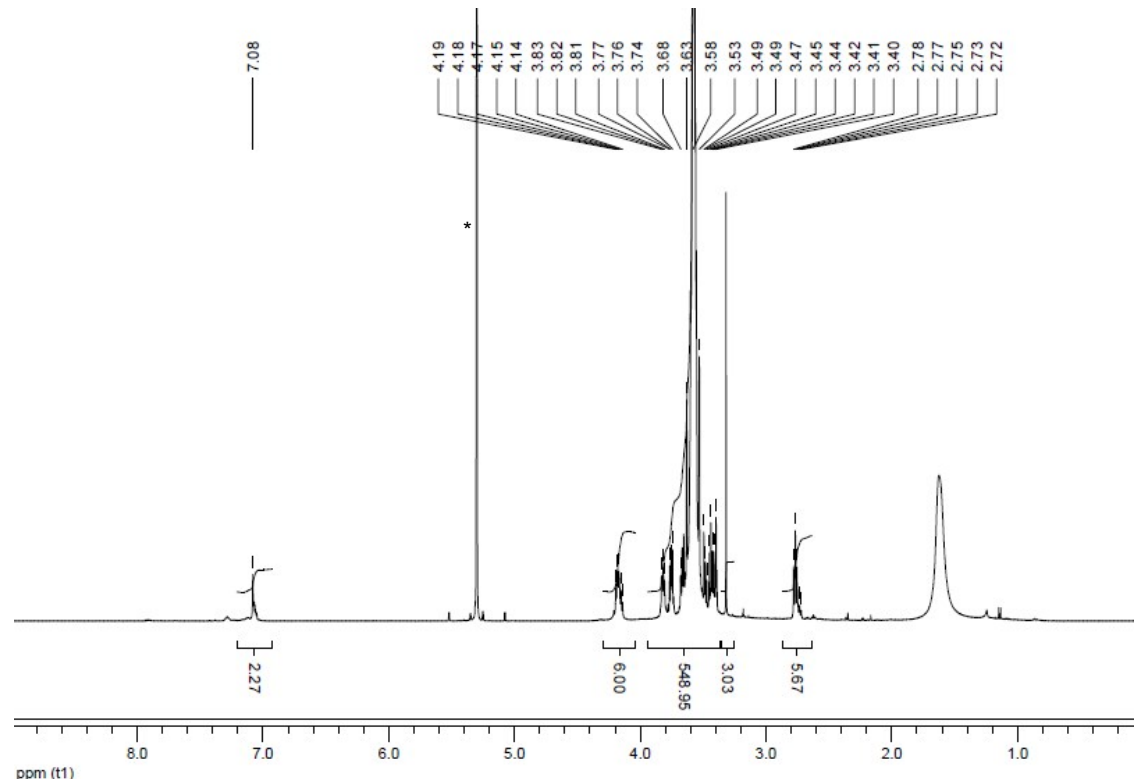


Figure S6. ¹H NMR spectrum of PEG-[G1]-NH₂

PEG-b[G2]-N₃(9)

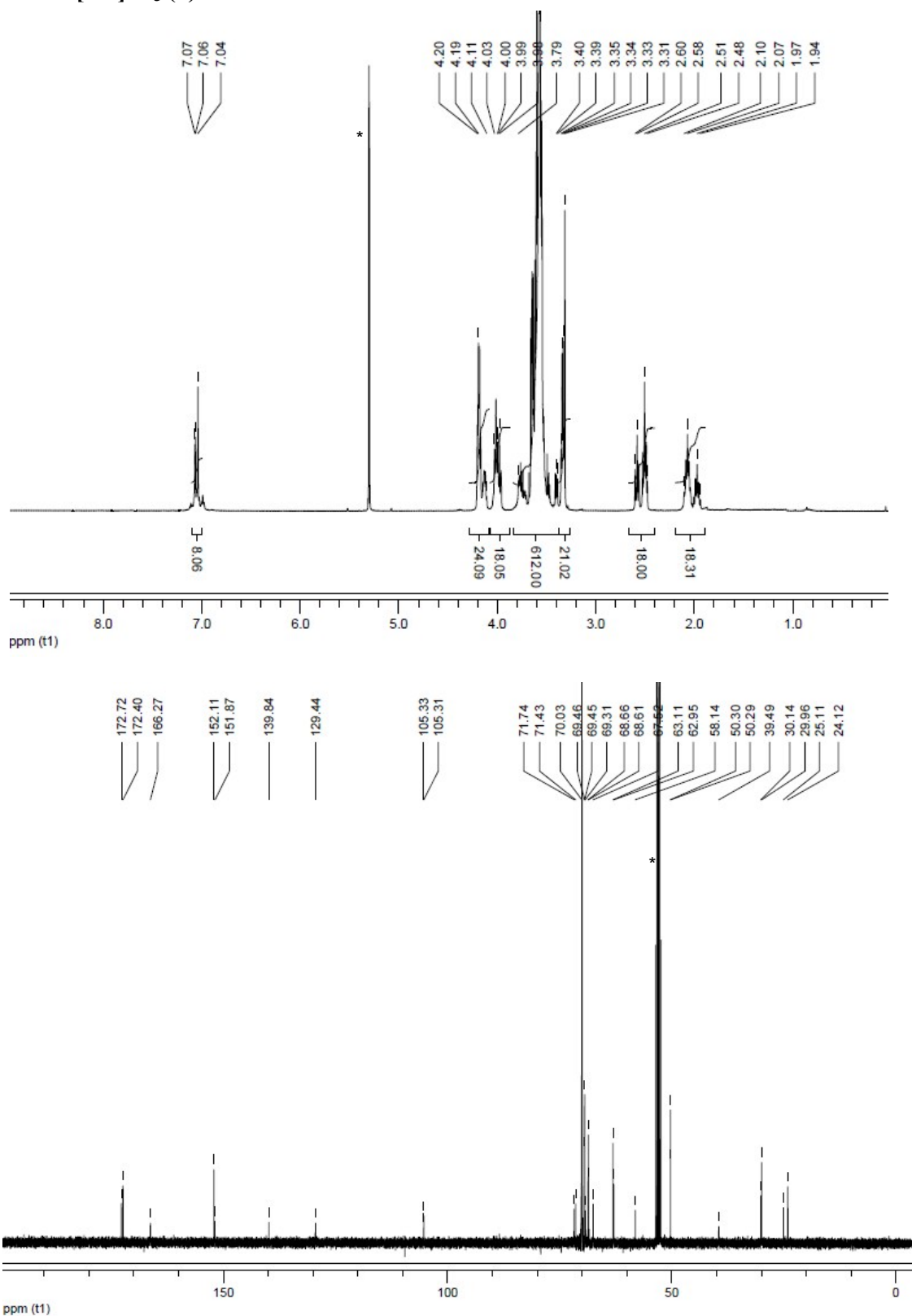


Figure S7. ¹H and ¹³C NMR spectra of PEG-b[G2]-N₃(9)

bD (12)

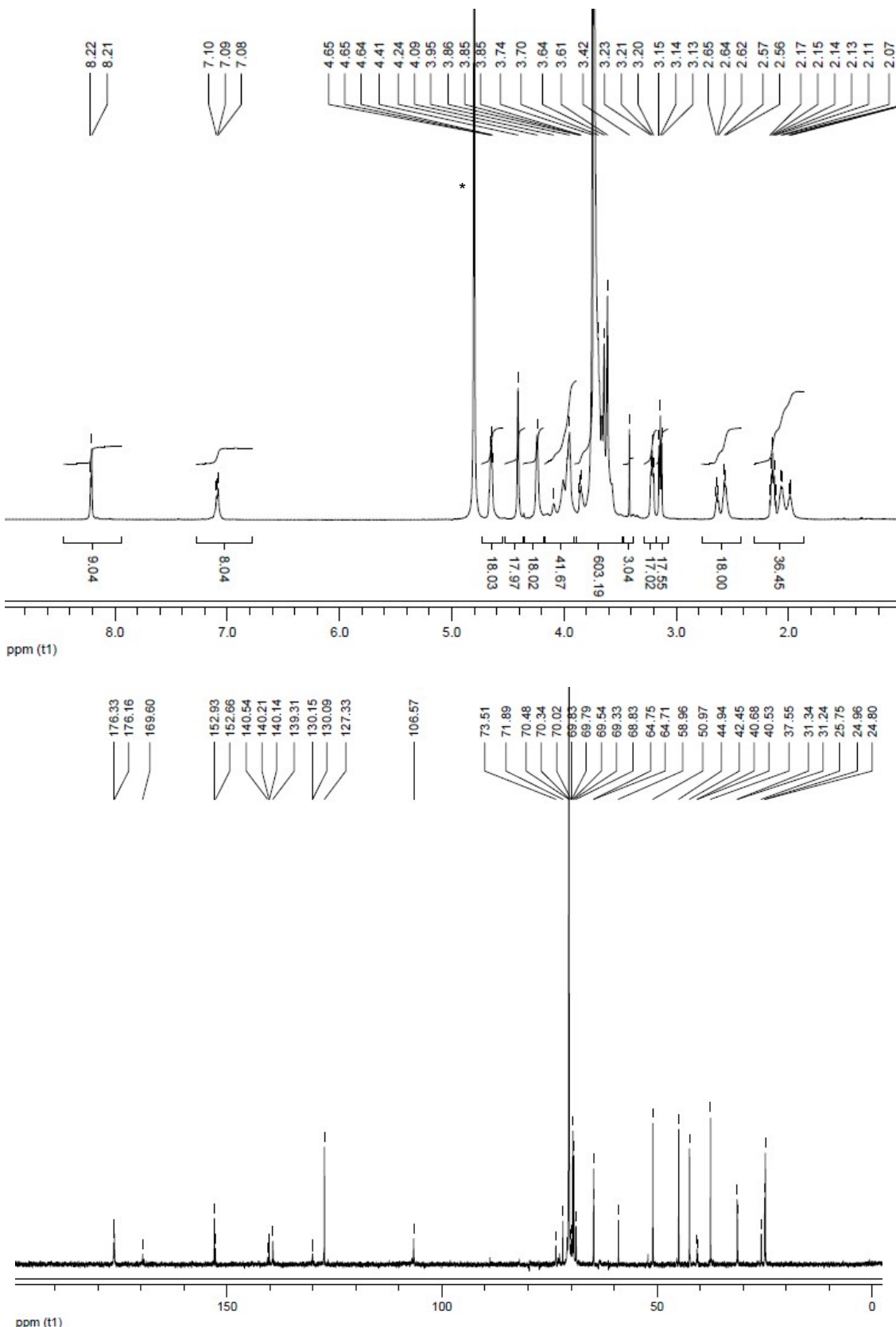


Figure S8. ^1H and ^{13}C NMR spectra of bD (12)

bB (13)

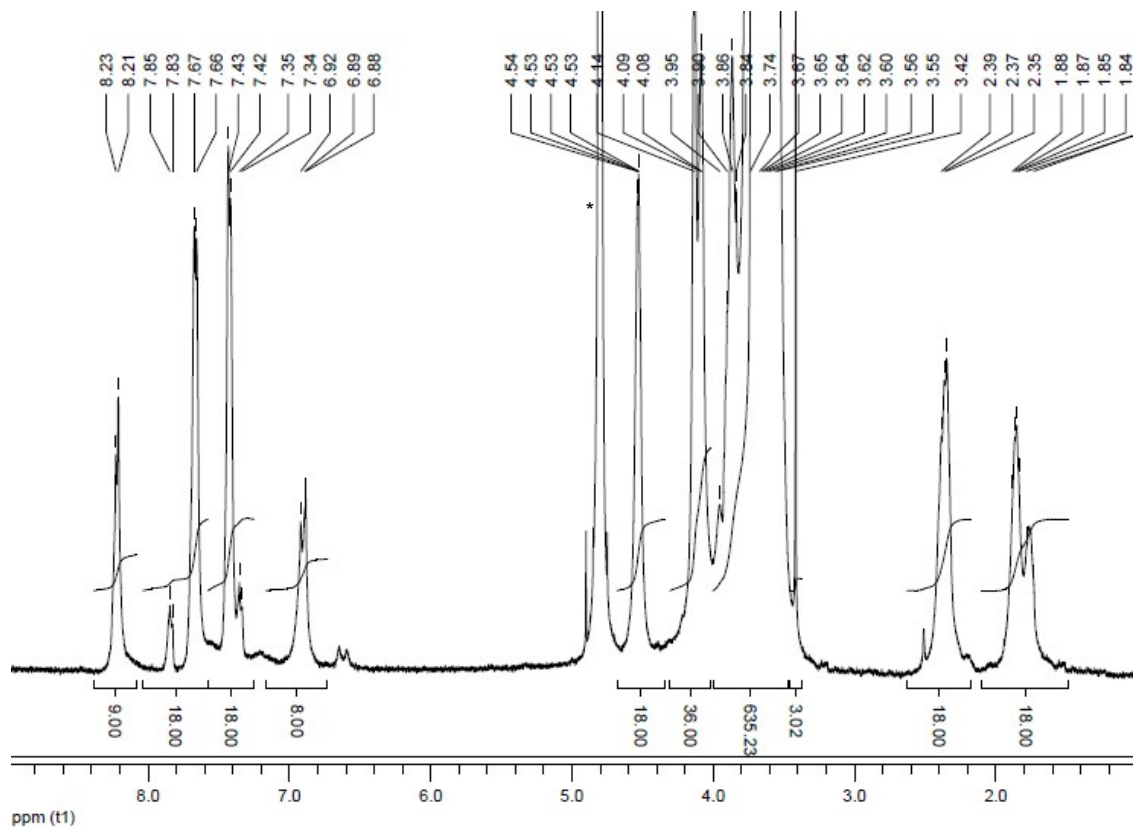


Figure S9. ^1H and ^{13}C NMR spectra of bB (13)

hsD (14)

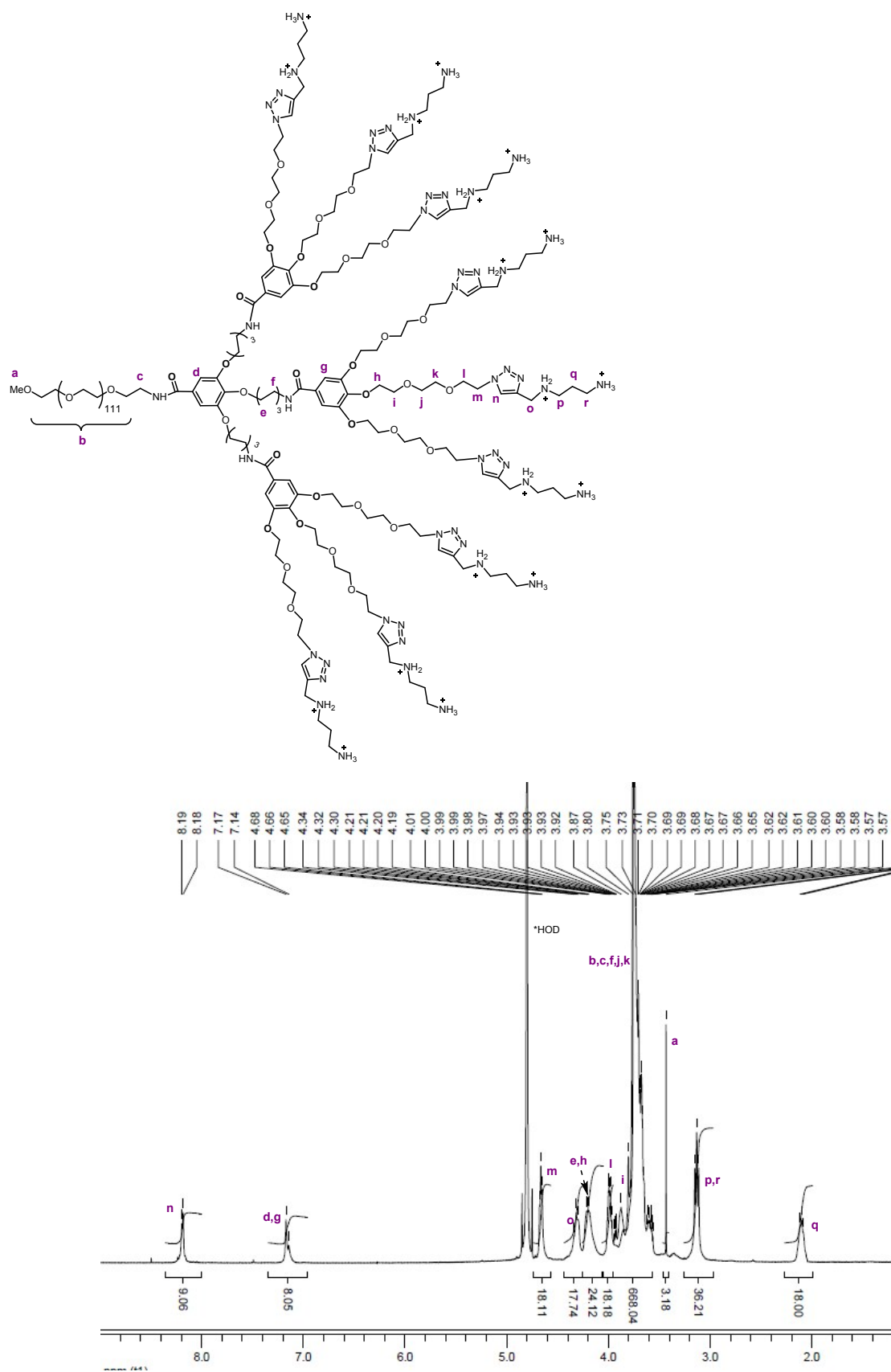


Figure S10. ^1H NMR spectrum and assignment of the signals for hsD (14)

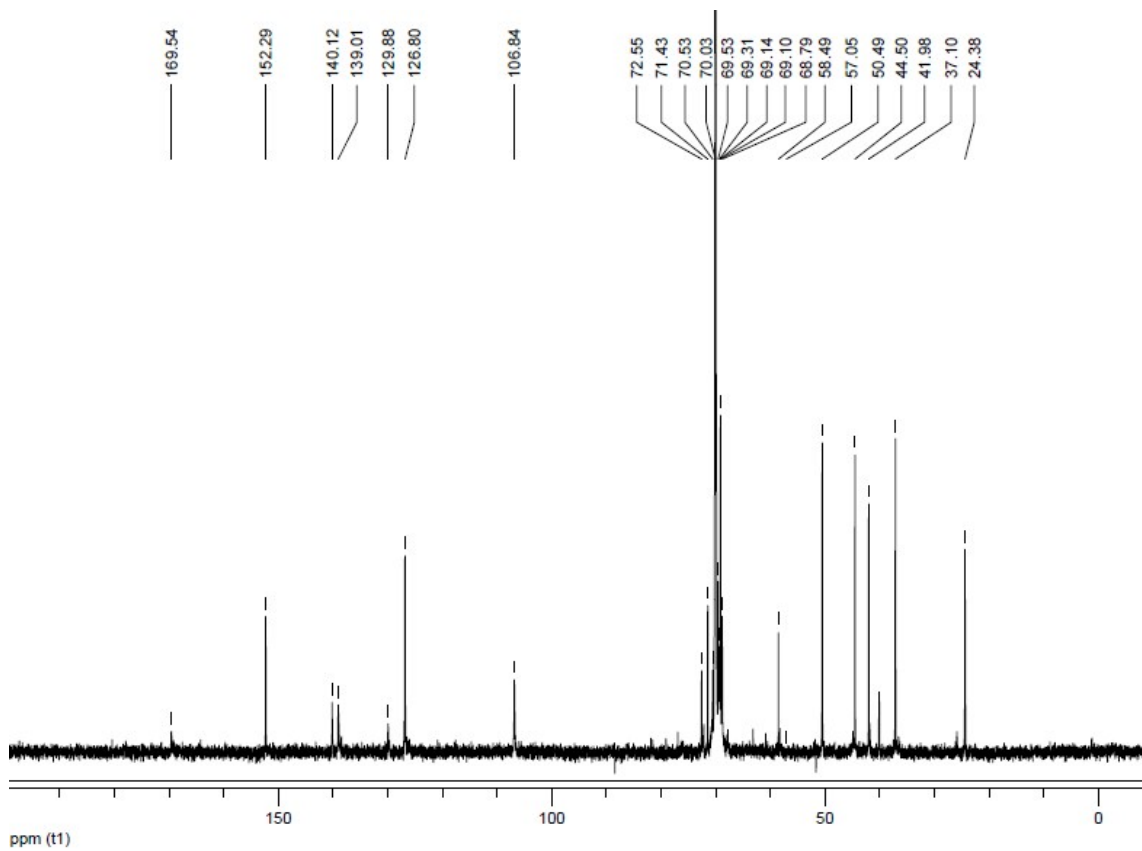


Figure S11. ¹³C NMR spectrum of hsD (14)

hsB (15)

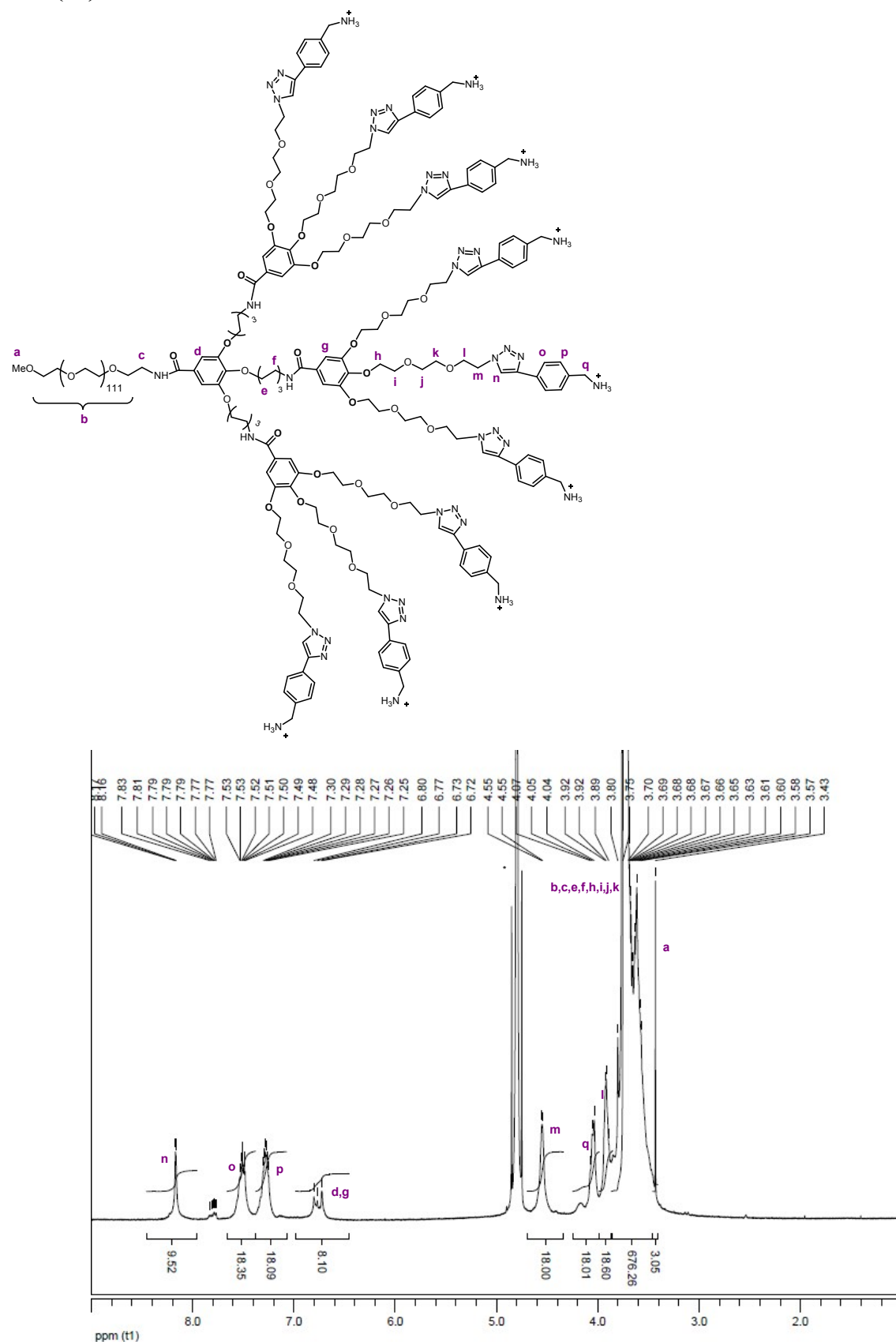


Figure S12. ^1H NMR spectrum and assignment of the signals for hsB (15)

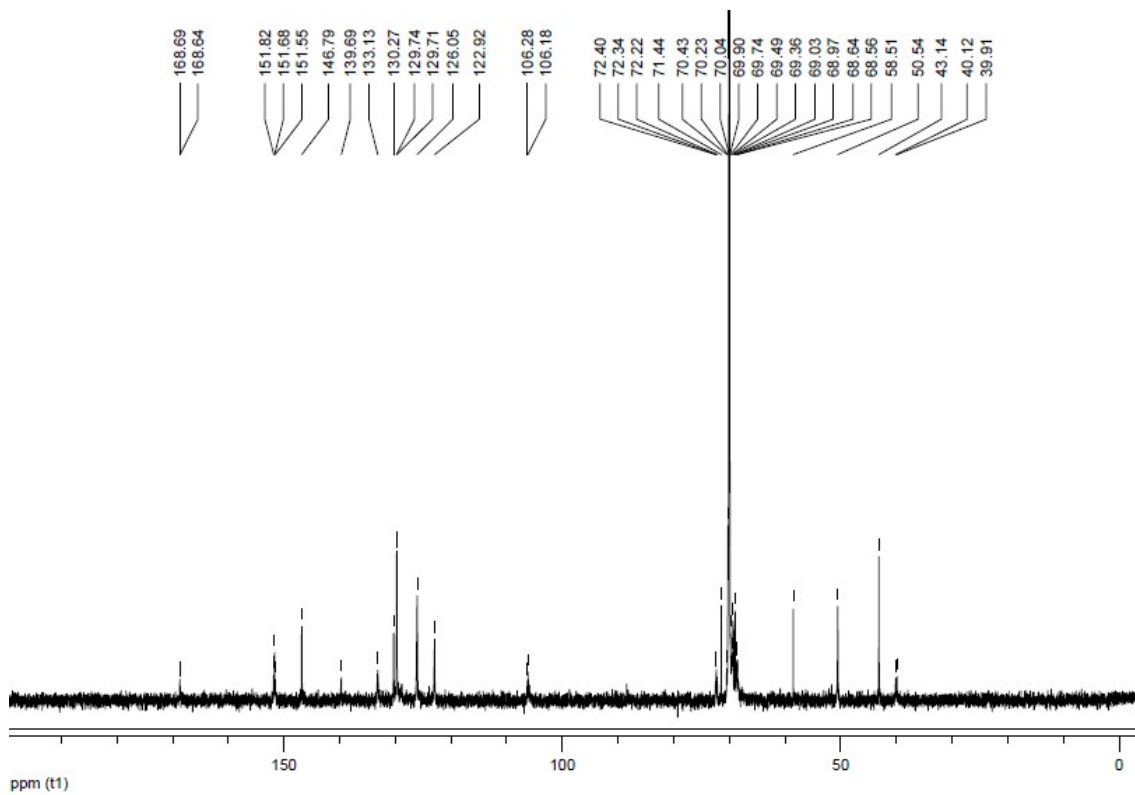
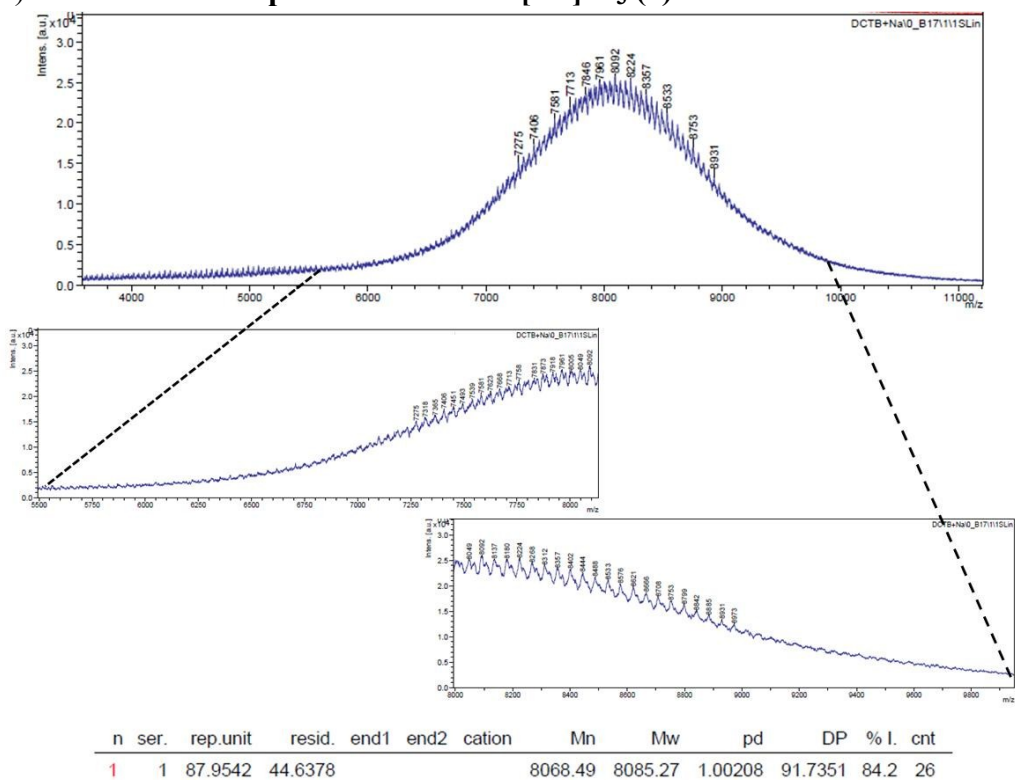


Figure S13. ^{13}C NMR Spectra of hsB (15)

2) MALDI-TOF Spectrum of PEG-b[G2]-N₃ (9)



Mn = 8068.49; Mw = 8085.27; PDI = 1.002

Figure S14. MALDI-TOF spectrum of PEG-b[G2]-N₃ (9)

3) FTIR Transmittance spectra

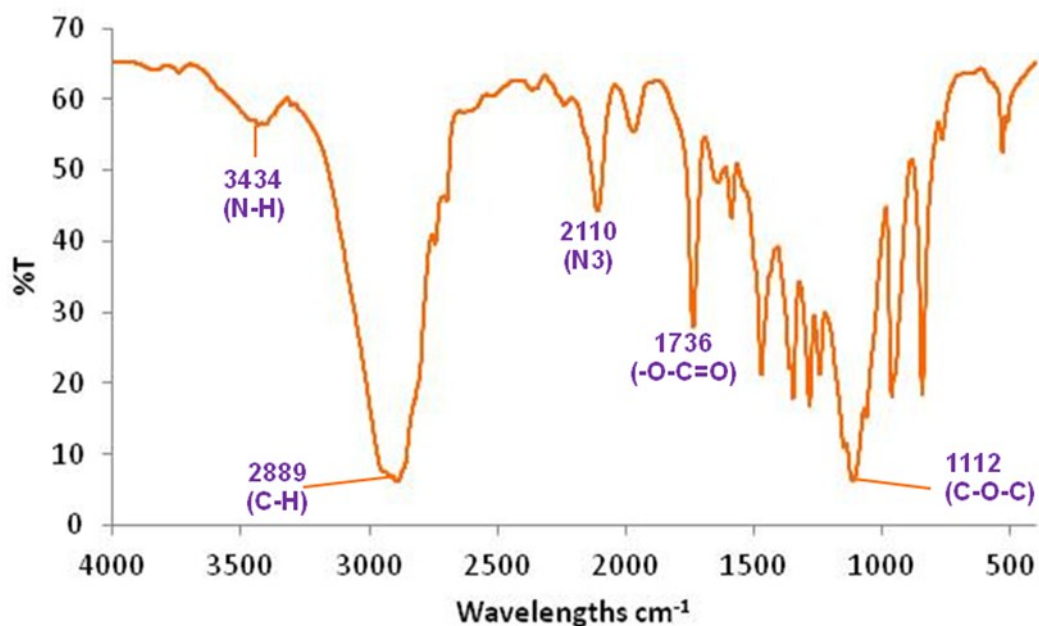


Figure S15. FTIR transmittance spectrum of PEG-b[G2]-N₃ (9) (KBr)

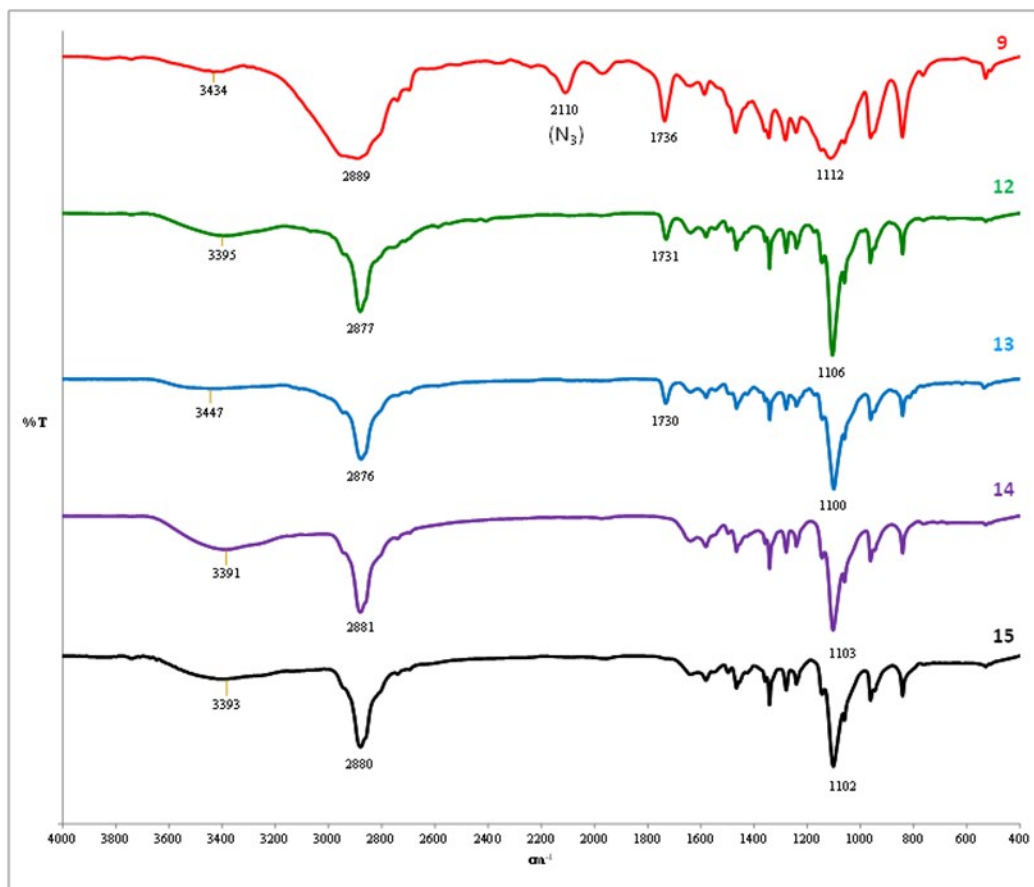


Figure S16. FTIR Transmittance spectra of PEG-b[G2]-N₃ (9), bD (12), bB (13), hsD (14) and hsB (15) (ATR)

4) Degradability Studies

Degradation of ammonium salt **6** was also studied at basic pH (pH 9.8) for comparison purposes. The ammonium salt **6** (1 mg/mL) was incubated at 37 °C in carbonate buffer saline (30 mM Na₂CO₃ + 420 mM NaCl, pD 9.8). Buffer was prepared in deuterium oxide and supplemented with acetone-d6 (D₂O/acetone-d6, 85:15) with the aim of improving solubility and resolution of NMR spectra for integration purposes. Sample was analyzed by ¹H-NMR at different time points.

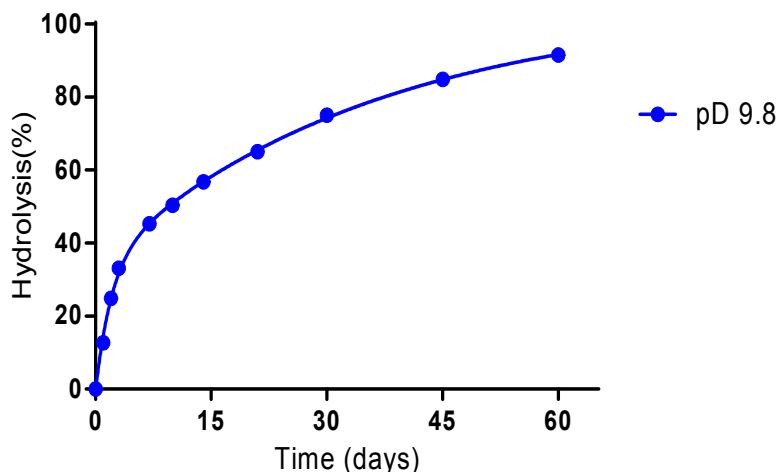


Figure S17. Kinetics of the ester hydrolysis in the amine-terminated unit **6** by ¹H NMR at pD 9.8.

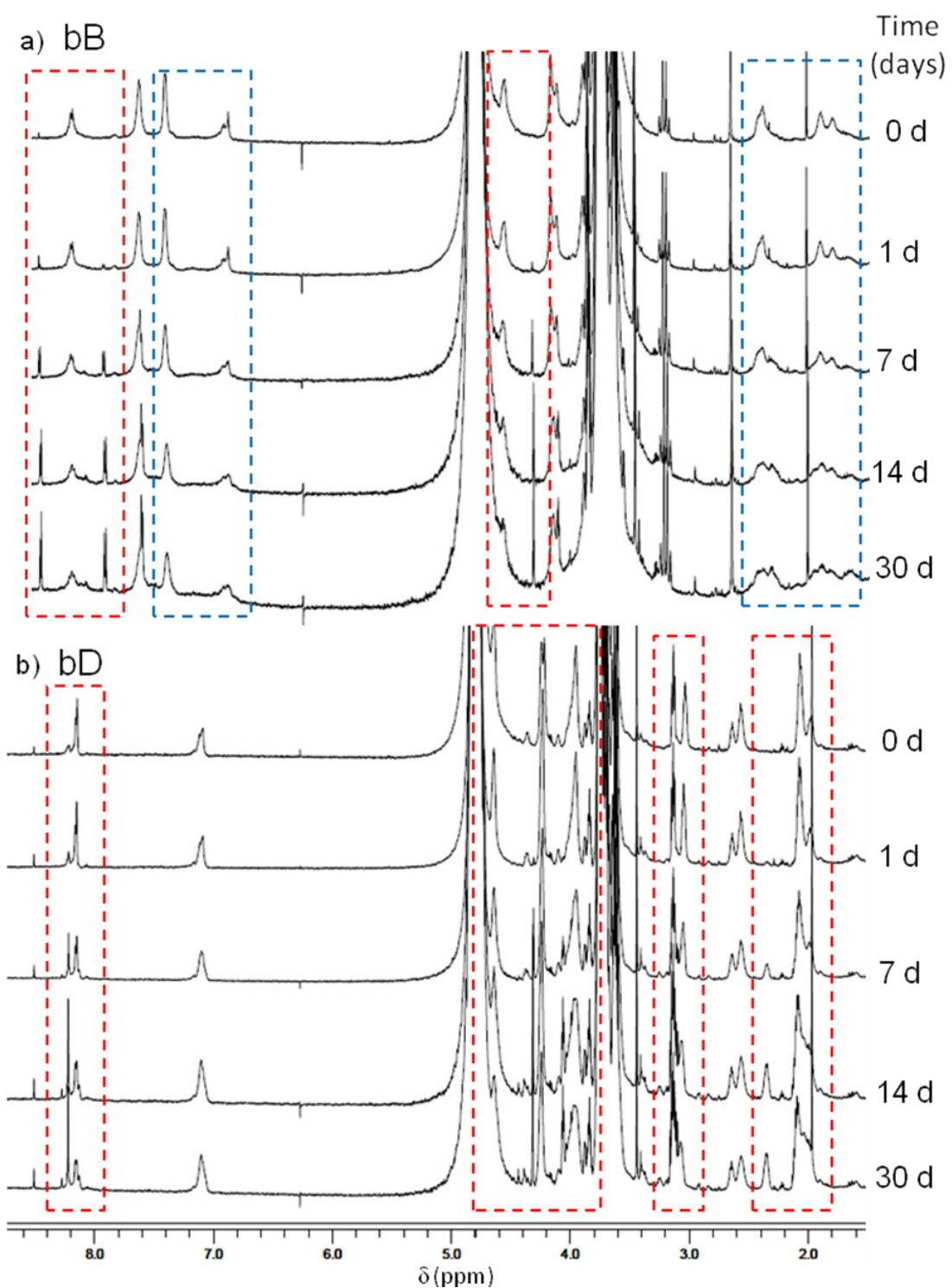


Figure S18. ^1H NMR spectra (600 MHz, D_2O , PBS 3x, pD 7.4) of amine-terminated bD (**12**) and bB (**13**) at different time points (0, 1, 7, 14 and 30 days). The most significant alterations observed on the spectra are highlighted with the dotted rectangles (in red – very important changes, including the appearance and/or disappearance of signals; in blue – important changes involving alterations on the signals intensity and/or shape).

5) Stability of the Dendriplexes in different media

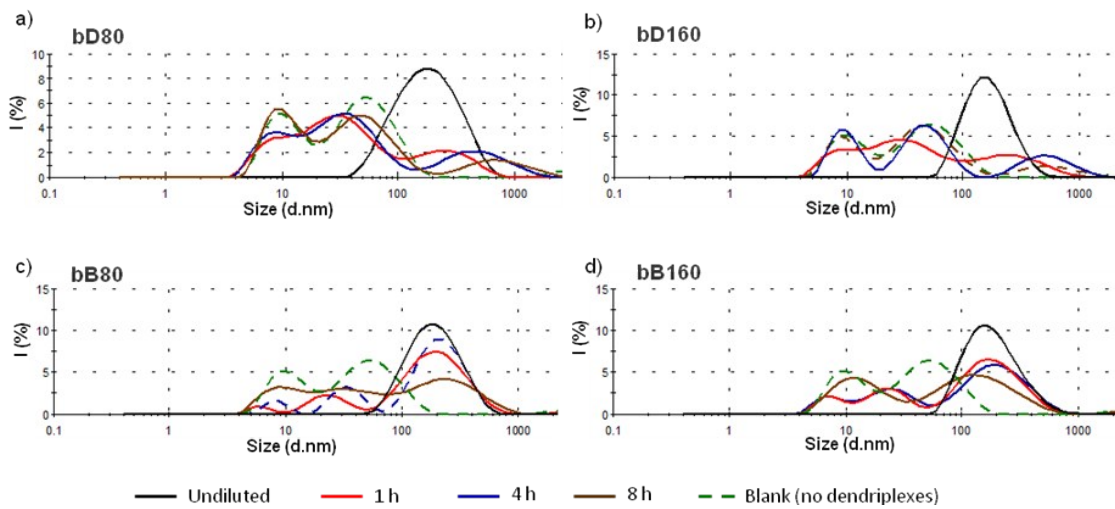
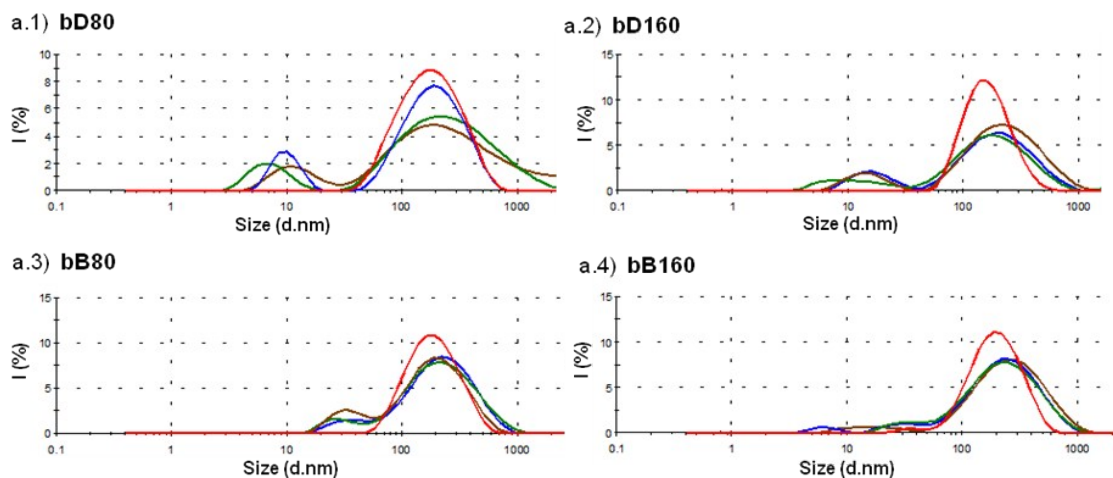
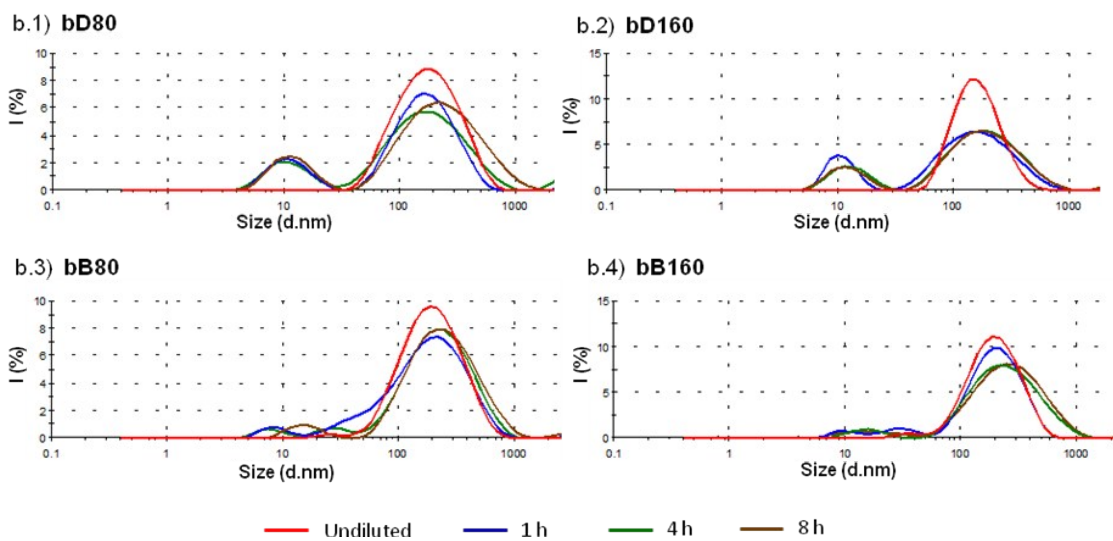


Figure S19. Stability of biodegradable dendriplexes in 1x PBS with 20% fetal bovine serum (FBS). a) bD (N/P 80); b) bD (N/P 160); c) bB (N/P 80); d) bB (N/P 160). Dendriplexes were formed at N/P 80 and 160, diluted 2-fold in PBS + 20 % FBS, and incubated for 1 h (red), 4 h (blue) and 8 h (brown), at 37 °C. Average size was then determined by DLS. Profile of PBS with FBS and no dendriplexes (Blank curve, in green) was taken in order to distinguish protein-related aggregates.

a) pH 5



b) pH 7.4



— Undiluted — 1 h — 4 h — 8 h

Figure S20. Stability of biodegradable dendriplexes at: a) pH 5.0 and b) pH 7.4. a.1) bD (N/P 80); a.2) bD (N/P 160); a.3) bB (N/P 80); a.4) bB (N/P 160); b.1) bD (N/P 80); b.2) bD (N/P 160); b.3) bB (N/P 80); b.4) bB (N/P 160). Dendriplexes were formed at N/P 80 and 160, diluted 2-fold in 10 mM NaOAc + 137 mM NaCl pH 5.0 and 1x PBS pH 7.4, and incubated for 1 h (blue), 4 h (green) and 8 h (brown), at 37 °C. Average size was then determined by DLS. Red curves represent the undiluted dendriplexes.

6) Heparin Dissociation Assay

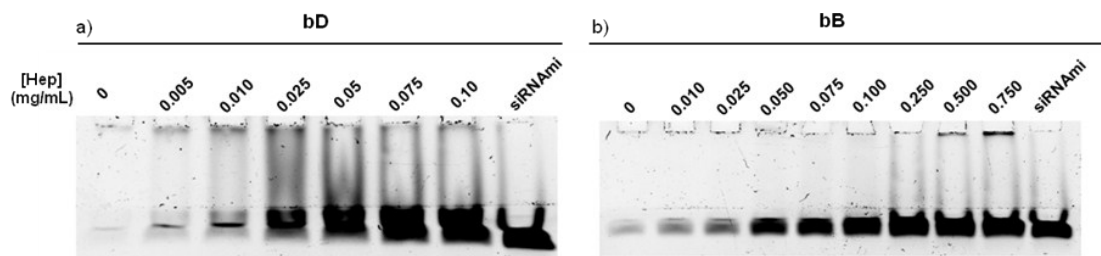


Figure S21. Heparin dissociation assay for: a) bD and b) bB dendriplexes. bD and bB dendriplexes at N/P 160 were incubated with increasing concentrations of heparin at 37 °C in physiological salt and pH conditions for 2 h. Samples were then run using PAGE to verify the extent of dissociated siRNAmi from the dendriplexes. In the siRNAmi lane the same amount of free siRNAmi as used for the preparation of the dendriplexes was loaded.

7) Dendriplexes degradation studies

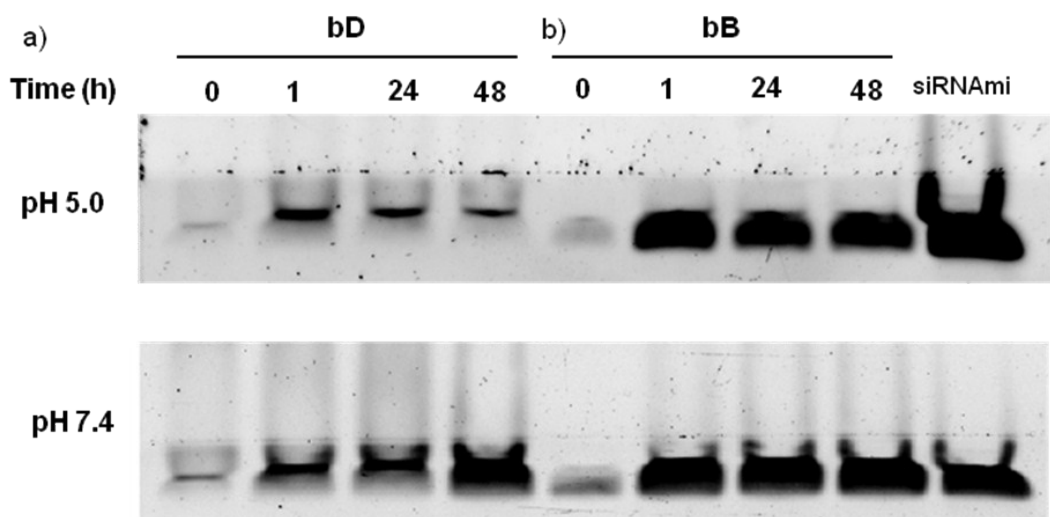


Figure S22. Degradation studies for: a) bD and b) bB siRNA dendriplexes. bD and bB at N/P 160 were incubated under acid (pH 5.0) and physiological pH (pH 7.4) conditions for 1, 24 and 48 h. Then, dendriplexes were incubated with heparin (at a final heparin concentration of 0.010 mg/mL and 0.025 mg/mL for bD and bB dendriplexes, respectively) for 2 h at 37 °C, in order to determine, in an indirect way, the amount of siRNA released with the time.

8) Internalization Data

Table S1. Percentage of cells with associated/internalized dendriplexes (positive cells) by flow cytometry

Treatment	N/P	% Positive Cells
NT		0.4
L2k		99.2
hsD	20	96.4
	40	98.8
	80	98.7
	160	99.3
bD	20	98.2
	40	98.2
	80	98.3
	160	98.2
hsB	20	98.3
	40	99.0
	80	99.1
	160	99.1
bB	20	98.1
	40	98.1
	80	98.2
	160	98.8

Table S2. Percentage of cells with internalized dendriplexes (positive cells) at N/P 160 by imaging flow cytometry

Treatment	% Positive Cells
NT	0.4
L2K	98.7
hsD	99.0
bD	94.6
hsB	99.8
bB	99.8

Table S3. Dendriplex-loaded vesicles (DLVs).

Copolymer	Dendriplex-loaded Vesicles (DLV)		
	Low (<1.5 spots)	Medium (1.5 – 5.5 spots)	High (>5.5 spots)
hsD	23 %	62 %	15 %
hsB	13 %	63 %	24 %
bD	16 %	51 %	33 %
bB	4 %	52 %	44 %

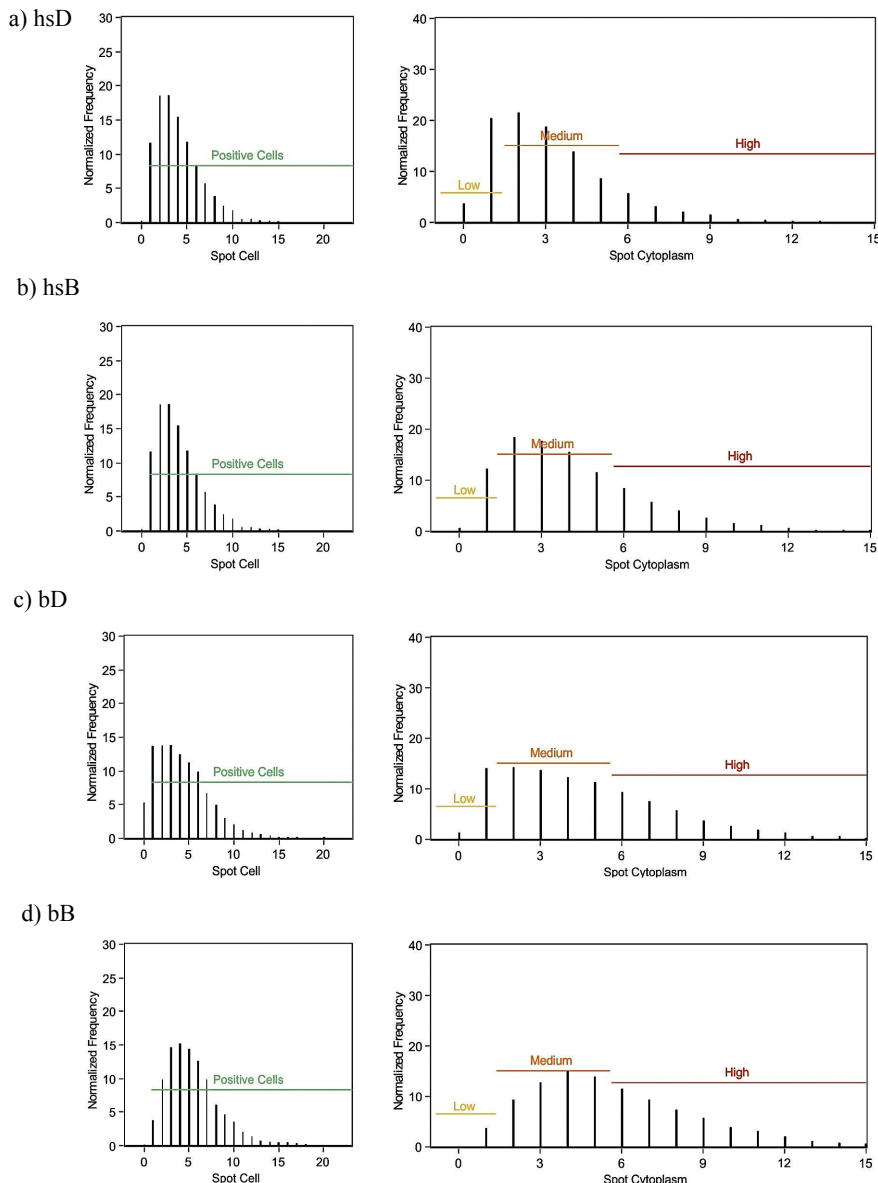


Figure S23. Dendriplex-loaded vesicles (DLV) per cell. a) hsD, b) hsB, c) bD, d) bB. Left column: Spot count for the cell mask. Right column: Spot count for the cytoplasm mask. Green: region for Cy-5 positive cells (membrane and cytoplasm); Low: region for low spot count cell (cytoplasm); Orange: region for medium spot count cells (cytoplasm); Red: region for high spot count cells (cytoplasm).